# DESIGN, SYTHESIS, CHARACTERIZATION, MOLECULAR DOCKING STUDIES, AND POSSIBLE BIOLOLOGICAL ACTIVITIES OF NOVEL PYRAZINE FUSED INDOLE DERIVATIVES.

**Tejaswini Kumari Dash[1]*, H.K.Sundeep Kumar[2], Mrityunjay Banerjee[3]**

**Abstract**

In an effort to develop safe and potent anti-diabetic and anticancer agents, a series of novel pyrazine fused Indole derivatives II-(4a-4l) was prepared. It was synthesized via Schiff's base with appropriately 2-aminopyrazine followed by n-benzoylation and Schiff's base with substituted benzaldehydes. All the synthesized compounds were performed characterized by IR, 1HNMR and MASS spectral analysis and evaluated for their antidiabetic and anticancer activities. Various molecular properties have been predicted by using Qikprop module (Table.No.2) and most of the compounds were beyond the recommended range. Based on the predicted ADME parameters, majority of the compounds had predicted CNS activity. Compounds **II-4d**, and **II-4j** had mostly inactive CNS activity. All the compounds except compounds **II-4d (94.2%)** and **II-4j (97.67%)** had 100% human oral absorption and most of the 10 compounds (II-4a to II-4l) were not permeable through skin. The molecular docking studies were performed in order to find the possible protein ligand interactions of the dataset ligands. Glide dock scores of the dataset ligands were shown in Table 4 along with the interaction of amino acids including their number. Among the docked ligands, dock scores of all the compounds ranged from **-9.2** (compound II-4c, II-4a) to **-5.2** (compound II-4k). Finally, the anticancer activity was found by brine shrimp lethality bioassay and allium cepa root tip meristem model. Anti-diabetic activity was carried out by glucose diffusion inhibitory study. From the results, the compound **II-4c (IC-50 value 47.82µg** for antidiabetic**) (38.01 µg/ml** for anticancer**)** exhibited good activities.

**Keywords:** Indole, Pyrazine, 2-aminopyrazine, Molecular docking, Anti-diabetic and Anticancer Activities.

[1]*Research Scholar(Pharmacy), Biju Patnaik University of Technology, Rourkela, Odisha, India-769004
[2,3] Professor in Pharmacy, Institute of Pharmacy and Technology, Salipur, India.

***Corresponding Author:** Tejaswini Kumari Dash
*Research Scholar, Biju Patnaik University of Technology, Rourkela, Odisha, India-769004

**DOI:** 10.48047/ecb/2023.12.si5a.0395

## INTRODUCTION:

Docking is widely used to anticipate the alignment of small molecule therapeutic compounds concerning their protein targets in anticipating the small molecule's affinity and activity.1 Docking plays a critical role in rational drug design. Considering the biological and pharmacological importance of docking studies, much effort has been made to improve the algorithms for docking prediction [1]. Docking is a mathematical technique that anticipates the preferable orientation of one molecule relative to another when they are linked together to create a stable complex. Using scoring functions, it is possible to estimate the strength of the connection or binding affinity across two compounds based on their preferential orientation. Indole chemically known as benzopyrole has become a popular topic due to its manifold uses.

The chemistry of Indole and its derivatives are particularly interesting because of their potential application [2-8] in medicinal chemistry as antitumor, antibacterial, antifungal, antiviral, antiparasitic, anti-tubercular, and insecticidal agents and also having anti-inflammatory, anti-diabetic properties. Moreover, Schiff's bases and its derivatives have played a crucial part in the development of theory of heterocyclic compounds, and also they used extensively in organic synthesis.

Studies on the properties and synthesis of hydrazones (imine/Schiff's bases) and their derivatives have shown that this class of compounds displays considerable biological activity and can be employed in the treatment of several diseases [9-12], especially cancer, malaria, Chagas disease, viral infections, leishmaniosis, Alzheimer'sDisease (AD), and bacterial and fungal infections, besides also displaying anti-inflammatory effect. Therefore, these molecules have great potential for applications in medicinal chemistry. Hydrazones are Schiff bases belonging to a class of compounds characterized by the skeleton $R_1R_2C=N-NR_3R_4$ that is featured in a variety of chemical and pharmacological applications. Their synthesis generally occurs by the condensation of hydrazine's with ketones or aldehydes, commonly requiring the use of an acid catalyst like glacial acetic acid. The new approach has targeted on the development of small biologically active molecules containing significant activity beyond toxicity related to the usual chemotherapy [13-14]. The Diabetes has been on ascent world over, but a major health problem and social burden in developing countries such as India. Over the years, different approaches have been used to improve how cytotoxic agents are designed, put through clinical trials and eventually released as commercially available drugs [15].

The aim of this study was to examine the effect of the electron donating or withdrawing groups at different positions of the aromatic ring at 3$^{rd}$ and 4$^{th}$ on cytotoxic properties and also to try to improve their solubility in water by introducing an imine and pyrazine ring group into the molecule. We synthesized a series of novel pyrazine fused Indole derivatives II-(4a-4l) was prepared. It was synthesized via Schiff's base with appropriately 2-aminopyrazine followed by n-benzoylation and Schiff's base with substituted benzaldehydes. All the synthesized compounds were performed characterized by IR, 1HNMR and MASS spectral analysis and evaluated for their antidiabetic and anticancer activities.

## EXPERIMENTAL SECTION

### Material and Methods:

The 2D structures of the series of novel pyrazine fused Indole derivatives II-(4a-4l) were converted to 3D using potential algorithms and high-efficient force fields. Initially geometrical optimization and energy minimization of molecules were performed by using the Ligprep tool of Schrodinger suite. Various ionization states were generated by Ligprep module using a special program EPIK along with various possible conformers and tautomer's. Molecular properties of the processed ligands were studied by using Qikprop module which predicts ADME profiles. The whole structure was minimized using OPLS-2005 force field using Protein Preparation by using AUTODOCK suite of MGL Tools. All chemicals of LR grade were used for synthesis, which were procured from Sigma-Aldrich, Merck, SD fine and Aware company.

The solvents of LR grade were used and purified before use. The Fourier-transform infrared spectroscopy (FT-IR) absorption spectra were obtained in the range 4000-400 cm-1 on Alpha Bruker FT-IR instrument. $^1$H Nuclear magnetic resonance (NMR) spectra were recorded on BrukerUx-NMR instrument and the samples was made in $CDCl_3$ using methyl silane (Me4Si) as the internal standard and chemical shifts were expressed in parts per million (PPM) and the melting point (MP) of the all the newly synthesized compounds were recorded on Metler Fp-51 instrument. The recoated Silica Gel G plates were used to found the progress of reaction as well as to assessment the purity of the compounds: n-Hexane: Ethyl acetate (7:3).

**Experimental Procedure.**

**General procedure:**

**Step: I: Synthesis of 1-(1H-indol-3-yl)-N-(pyrazine-2-yl) methanimine (2a).** Indole-3-carbaldehyde (1a) was taken in a mixture of 2-aminopyrazine (0.01 mole), glacial acetic acid (5ml) and ethanol 30 ml in round bottom flask. Then the reaction mixture was refluxed for 2-3 hrs. The progress of the reaction was monitored by TLC (n-hexane: Ethyl acetate) (8:2). The reaction mixture was cooled to room temperature. A solid was obtained, which was filtered off, washed with hexane and recrystallized from methanol to give crystalline solid.

**Step: II: Synthesis of (4-aminophenyl) (3-{(pyrazine-2-yl)imino]methyl}-1H-ndol-1-yl)-methanone.** In the round bottomed flask take 1-(1H-indol-3-yl)-N-(pyrazine-2-yl) methanimine (2a) (3.37mM) and equimolar quantity of 4-amino benzoyl chloride (3.7mM), mix with 20ml of DMF and to this mixture add 2gm of $K_2CO_3$. After gentle mixing of this reaction mixture, reflux for 2 hr, cool and pour to 100 ml of ice cold water. The resultant orange red ppt. collected wash with water and dried and recrystallized from acetonitrile.

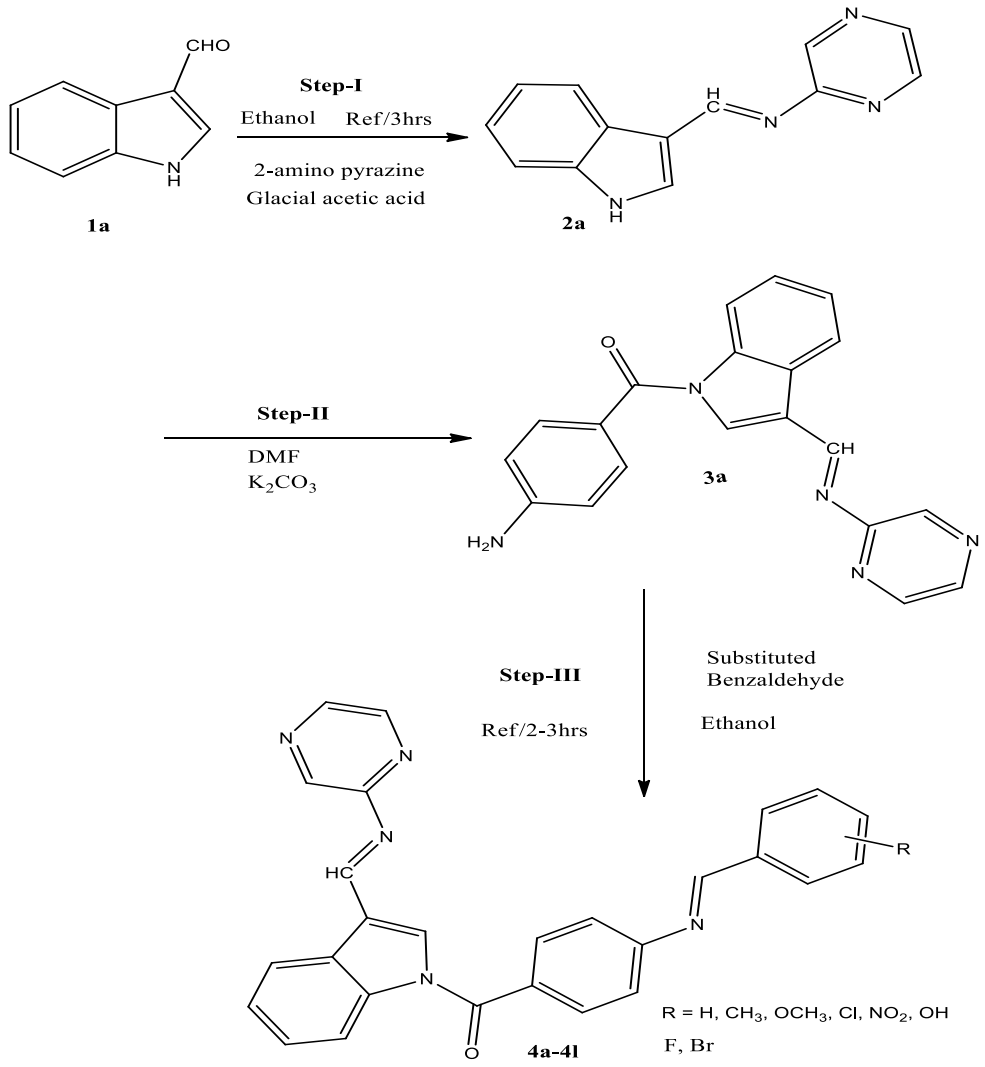


**Figure no.1: Scheme**

**Step: III. Synthesis of (4-{(E)}-4-phenyl-methylidene]amino}phenyl)(3-{(E)-[pyrazine-2yl)imino] methyl}-1H-indol-1-yl)methanone [II-4a-4j].** The (4-aminophenyl)(3-{(pyrazine -2-yl)imino]methyl}-1H-ndol-1-yl)-methanone (3a) was taken in a mixture of substituted benzaldehyde (0.01 mole), glacial acetic acid (5ml) and ethanol 30 ml in round bottom flask. Then the reaction mixture was refluxed for 2-3 hrs. The progress of the reaction was monitored by TLC (n-hexane: Ethyl acetate) (7:3). The reaction mixture was cooled to room temperature. A solid was obtained, which was filtered off, washed with hexane and recrystallized from methanol to give crystalline solid.

**Table no.1:** Physical data II-4a-4l

| Compounds | Molecular Formula | R | Molecular weight(gm) | M.P($^0$C) | %Yield |
|---|---|---|---|---|---|
| **II-4a** | $C_{29}H_{19}ClFBrN_50_3$ | H | 429.16 | 137-139 | 79.04 |
| **II-4b** | $C_{29}H_{19}ClFBrN_50_3$ | 4-$CH_3$ | 443.17 | 166-168 | 81.76 |
| **II-4c** | $C_{29}H_{19}ClFBrN_50_3$ | 4-$OCH_3$ | 459.17 | 201-203 | 84.13 |
| **II-4d** | $C_{29}H_{19}ClFBrN_50_3$ | 4-Cl | 463.12 | 217-219 | 81.13 |
| **II-4e** | $C_{29}H_{19}ClFBrN_50_3$ | 4-F | 447.15 | 119-121 | 76.32 |
| **II-4f** | $C_{29}H_{19}ClFBrN_50_3$ | 4-Br | 507.07 | 251-253 | 75.09 |
| **II-4g** | $C_{29}H_{19}ClFBrN_50_3$ | 4-$NO_2$ | 474.14 | 208-211 | 84.04 |
| **II-4h** | $C_{29}H_{19}ClFBrN_50_3$ | OH | 445.15 | 223-225 | 86.09 |
| **II-4i** | $C_{29}H_{19}ClFBrN_50_3$ | 3-$NO_2$ | 474.14 | 231-233 | 73.05 |
| **II-4j** | $C_{29}H_{19}ClFBrN_50_3$ | 3,4-$(OCH_3)_2$ | 489.18 | 257-269 | 79.04 |
| **II-4k** | $C_{29}H_{19}ClFBrN_50_3$ | 3-OH | 445.15 | 229-231 | 81.63 |
| **II-4l** | $C_{29}H_{19}ClFBrN_50_3$ | 3-Cl | 463.12 | 233-235 | 86.43 |

**Compound.II-4a:(4-{(E)}-4-phenyl-methylidene]amino}phenyl)(3-{(E)-[pyrazine-2yl) imino]methyl}-1H-indol-1-yl)methanone:** M.P. 137-139$^o$C, Mol. Formula: $C_{27}H_{19}N_5O$, Yield. 79.04%. IR ($\nu$ cm−1): 3053(C-H *Str*, Aromatic), 2972, 2829(C-H *Str*, Aliphatic), 1709(-CO Str, NC=O methanone), 1622(C=N, *Str*), 1551(C=CH *Str*), 1389(C=C *Str*), 1053(C-N, *Str*). $^1$H-NMR (DMSO) $\delta\delta$ ppm: 9.5542(s, 1H, Imine proton), 9.3093(s, 1H, Imine proton), 7.9032(s, 1H, Pyrazine proton); 7.9023(d, 2H, Ar-H), 7.7328(d, 2H, Ar-H), 7.7234-7.7198(d, 2H, Ar-H), 7.6564-7.6453(d, 2H, Ar-H), 7.5213-7.5003(t, 2H, Ar-H), 7.4231-7.4054(t, 3H, Ar-H); 7.0021(s, 1H, Indole proton). Mass (LC-MS): m/z 429.16(M), 430.32(M + 1, 100%).

**Compound.II-4b:(4-{(E)}-[4-methylphenyl) methylidene]amino}phenyl)(3-{(E)-[pyrazine-2yl)imino] methyl}-1H-indol-1-yl)methanone:** M.P. 166-168$^o$C, Mol. Formula: $C_{28}H_{21}N_5O$, Yield.81.76%. IR ($\nu$ cm−1): 3056(C-H *Str*, Aromatic), 2956(C-H *Str*, Aliphatic), 1705(-CO Str, NC=O methanone), 1636(C=N, *Str*), 1538 (C=CH *Str*), 1309(C=C *Str*), 1048(C-N, *Str*). $^1$H-NMR (DMSO) $\delta\delta$ ppm: 9.3352(s, 1H, Imine proton), 9.1054(s, 1H, Imine proton), 8.4021(s, 1H, Pyrazine proton); 7.9463-7.9387(d, 2H, Ar-H), 7.8362-7.8210(d, 2H, Ar-H), 7.7653-7.7543(d, 2H, Ar-H), 7.7123-7.7022(d, 2H, Ar-H), 7.6636-7.6332(d, 2H, Ar-H),7.5563-7.5342(t, 2H, Ar-H); 7.3983(t, 2H, Ar-H); 7.3908(s, 1H, Indole proton); 1.9032(s, 3H, Ar-$CH_3$). Mass (LC-MS): m/z 443.17(M), 444.21(M + 1, 100%).

**Compound.II-4c:(4-{(E)}-[4-methoxyphenyl) methylidene]amino}phenyl)(3-{(E)-[pyrazine -2yl) imino] methyl}-1H-indol-1-yl)methanone:** M.P. 201-203$^o$C, Mol. Formula: $C_{28}H_{21}N_5O_2$, Yield.84.13%. IR ($\nu$ cm−1): 3159(C-H *Str*, Aromatic), 2982(C-H *Str*, Aliphatic), 1725(-CO Str, NC=O methanone), 1567(C=N, *Str*), 1486(C=CH *Str*), 1397(C=C *Str*), 1026(C-N, *Str*). $^1$H-NMR (DMSO) $\delta\delta$ ppm: 9.8874(s, 1H, Imine proton), 9.5532(s, 1H, Imine proton), 8.0876(s, 1H, Pyrazine proton); 7.8123-7.8032(d, 2H, Ar-H), 7.7998-7.7803(d, 2H, Ar-H), 7.7634-7.6309(d, 2H, Ar-H), 7.5123-7.5043(d, 2H, Ar-H), 7.5008(d, 2H, Ar-H), 7.4954(t, 2H, Ar-H); 7.3904-7.3894(t, 2H, Ar-H); 6.9908(s, 1H, Indole proton); 3.6564(s, 3H, Ar-$OCH_3$). Mass (LC-MS): m/z 459.17(M), 460.12 (M + 1, 100%).

**Compound.II-4d:(4-{(E)}-[4-chlorophenyl) methylene]amino} phenyl)(3-{(E)-[pyrazine -2yl)imino] methyl}-1H-indol-1-yl)methanone:** M.P. 217-219$^o$C, Mol. Formula: $C_{27}H_{18}N_5OCl$, Yield.81.13%. IR ($\nu$ cm−1): 3029(C-H *Str*, Aromatic), 2899(C-H *Str*, Aliphatic), 1710(-CO Str, NC=O methanone), 1612(C=N, *Str*), 1550 (C=CH *Str*), 1450(C=C *Str*), 1116(C-N, *Str*); 810(-Cl *Str*, Ar-Cl). $^1$H-NMR (DMSO) $\delta\delta$ ppm: 9.8832(s, 1H, Imine proton), 9.3342(s, 1H, Imine proton), 8.3354(s, 1H, Pyrazine proton); 8.0982-8.0763(d, 2H, Ar-H), 7.9093-7.9002(d, 2H, Ar-H), 7.9124(s, 1H, Indole proton);7.8032(d, 2H, Ar-H), 7.8002(d, 2H, Ar-H), 7.7930-7.7732(d, 2H, Ar-H), 7.3092-7.2983(d, 2H, Ar-H); 6.8904-6.8673(t, 2H, Ar-H). Mass (LC-MS): m/z 463.12(M), 464.21(M + 1, 100%), 465.21(M+2, 30%).

**Compound.II-4e:(4-{(E)}-[4-florophenyl) methylidene]amino}phenyl)(3-{(E)-[pyrazine-2yl)imino] methyl} -1H-indol-1-yl)methanone:** M.P. 119-121$^o$C, Mol. Formula: $C_{27}H_{18}N_5OF$, Yield. 76.32%. IR ($\nu$ cm−1): 3098(C-H *Str*, Aromatic), 2894(C-H *Str*, Aliphatic), 1721(-CO Str, NC=O methanone), 1604(C=N, *Str*), 1532(C=CH *Str*), 1421(C=C *Str*), 1098(C-N, *Str*); 832(-C-F *Str*, Ar-F). $^1$H-NMR (DMSO) $\delta\delta$ ppm: 9.6754(s, 1H, Imine proton), 9.4934(s, 1H, Imine proton), 8.2012(s, 1H, Pyrazine proton); 8.1023-8.1009(d, 2H, Ar-H), 7.9654-7.9032(d, 2H, Ar-H), 7.8022(s, 1H, Indole proton);7.7843-7.7003(d, 2H,

Ar-H), 7.6853-7.6120(d, 2H, Ar-H), 7.5352-7.5002(d, 2H, Ar-H), 7.4032-7.3323(d, 2H, Ar-H); 7.1022-7.0993(t, 2H, Ar-H). Mass (LC-MS): m/z 447.15(M), 448.09(M + 1, 100%), 449.05(M+2, 30%).

**Compound.II-4f:(4-{(E)}-[4-bromophenyl) methylidene]amino}phenyl)(3-{(E)-[pyrazine -2yl)imino] methyl}-1H-indol-1-yl)methanone:** M.P. 251-253ºC, Mol. Formula: $C_{27}H_{18}N_5OBr$, Yield.75.09%. IR ($\nu$ cm−1): 3084(C-H *Str*, Aromatic), 2984(C-H *Str*, Aliphatic), 1721(-CO Str, NC=O methanone), 1603(C=N, *Str*), 1543 (C=CH *Str*), 1421(C=C *Str*), 1093(C-N, *Str*); 835(-C-Br *Str*, Ar-Br). $^1$H-NMR (DMSO) $\delta\delta$ ppm: 9.6843(s, 1H, Imine proton), 9.2874(s, 1H, Imine proton), 8.4532(s, 1H, Pyrazine proton); 8.2324-8.1543(d, 2H, Ar-H), 7.8793-7.7643(d, 2H, Ar-H), 7.6754(s, 1H, Indole proton);7.5643(d, 2H, Ar-H), 7.4983(d, 2H, Ar-H), 7.3764(d, 2H, Ar-H), 7.2019-7.2002(d, 2H, Ar-H); 6.9983-6.9023(t, 2H, Ar-H). Mass (LC-MS): m/z 507.07(M), 508.32(M + 1, 100%), 409.09(M+2, 30%).

**Compound.II-4g:(4-{(E)}-[4-nitrophenyl) methylidene]amino}phenyl)(3-{(E)-[pyrazine -2yl)imino]methyl}-1H-indol-1-yl)methanone:** M.P. 208-211ºC, Mol. Formula: $C_{27}H_{18}N_6O_3$, Yield.84.04%. IR ($\nu$ cm−1): 3067(C-H *Str*, Aromatic), 2994(C-H *Str*, Aliphatic), 1717(-CO Str, NC=O methanone), 1639(-$NO_2$ *Str* in Ar-$NO_2$); 1612(C=N, *Str*), 1503(C=CH *Str*), 1418(C=C *Str*), 1087(C-N, *Str*). $^1$H-NMR (DMSO) $\delta\delta$ ppm: 9.5874(s, 1H, Imine proton), 9.4533(s, 1H, Imine proton), 8.3823(s, 1H, Pyrazine proton); 8.2093-8.1092(d, 2H, Ar-H), 7.9843-7.9032(d, 2H, Ar-H), 7.7843(s, 1H, Indole proton); 7.6743-7.6142(d, 2H, Ar-H), 7.5094(d, 2H, Ar-H), 7.4032-7.3984(d, 2H, Ar-H), 7.2234-7.2182(d, 2H, Ar-H); 6.8743-6.7833(t, 2H, Ar-H). Mass (LC-MS): m/z 474.14(M), 475.34(M + 1, 100%).

**Compound.II-4h:(4-{(E)}-[4-hydroxyphenyl) methylidene]amino}phenyl)(3-{(E)-[pyrazine -2yl)imino]methyl}-1H-indol-1-yl)methanone:** M.P. 223-225ºC, Mol. Formula: $C_{27}H_{19}N_5O_2$, Yield.86.09%. IR ($\nu$ cm−1): 3543(-OH *Str* in Ar-OH); 3094(C-H *Str*, Aromatic), 2998(C-H *Str*, Aliphatic), 1720(-CO *Str*, NC=O methanone); 1609(C=N, *Str*), 1521(C=CH *Str*), 1404(C=C *Str*), 1032(C-N, *Str*). $^1$H-NMR (DMSO) $\delta\delta$ ppm: 9.6743(s, 1H, Imine proton), 9.3092(s, 1H, Imine proton), 8.2983(s, 1H, Pyrazine proton); 8.1092-8.0983(d, 2H, Ar-H), 7.8973-7.8102(d, 2H, Ar-H), 7.6744(s, 1H, Indole proton); 7.5433-7.5021(d, 2H, Ar-H), 7.4321(d, 2H, Ar-H), 7.2093-7.1943(d, 2H, Ar-H), 7.0943-7.0032(d, 2H, Ar-H); 6.7843-6.6743(t, 2H, Ar-H). Mass (LC-MS): m/z 445.15(M), 446.32(M + 1, 100%).

**Compound.II-4i:(4-{(E)}-[3-nitrophenyl) methylidene]amino}phenyl)(3-{(E)-[pyrazine -2yl)imino]methyl}-1H-indol-1-yl)methanone:** M.P. 231-233ºC, Mol. Formula: $C_{27}H_{18}N_6O_3$, Yield. 73.16%. IR ($\nu$ cm−1): 3087(C-H *Str*, Aromatic), 2989(C-H *Str*, Aliphatic), 1710(-CO Str, NC=O methanone), 1621(-$NO_2$ *Str* in Ar-$NO_2$); 1614(C=N, *Str*), 1512(C=CH *Str*), 1424 (C=C *Str*), 1078(C-N, *Str*). $^1$H-NMR (DMSO) $\delta\delta$ ppm: 9.6543(s, 1H, Imine proton), 9.3984(s, 1H, Imine proton), 8.2983(s, 1H, Pyrazine proton); 8.2132-8.2093(d, 2H, Ar-H), 8.0342(s, 1H, Ar-H); 7.9763-7.9563(d, 2H, Ar-H), 7.80322(s, 1H, Indole proton); 7.5873-7.4232(d, 2H, Ar-H), 7.3894-7.2873(d, 2H, Ar-H), 7.2133-7.2002(d, 2H, Ar-H), 7.1232-7.1084(t, 2H, Ar-H). Mass (LC-MS): m/z 474.14(M), 475.34(M + 1, 100%).

**Compound.II-4j:(4-{(E)}-[3,4-dimethoxyphenyl)methylidene]amino}phenyl)(3-{(E)-[pyrazine-2yl)imino]methyl}-1H-indol-1-yl) methanone:** M.P. 257-259ºC, Mol. Formula: $C_{29}H_{23}N_5O_3$, Yield. 79.04%. IR ($\nu$ cm−1): 3076(C-H *Str*, Aromatic), 2978(C-H *Str*, Aliphatic), 1721(-CO Str, NC=O methanone); 1619(C=N, *Str*), 1532(C=CH *Str*), 1442(C=C *Str*), 1098C-N, *Str*). $^1$H-NMR (DMSO) $\delta\delta$ ppm: 9.7843(s, 1H, Imine proton), 9.2091(s, 1H, Imine proton), 8.3092(s, 1H, Pyrazine proton); 8.1879-8.1003(d, 2H, Ar-H), 7.9983(s, 1H, Ar-H); 7.8120-7.8003(d, 2H, Ar-H), 7.7893(s, 1H, Indole proton); 7.6754-7.6005(d, 2H, Ar-H), 7.2983-7.2094(d, 2H, Ar-H), 7.1092(d, 2H, Ar-H), 6.9084-6.8943(t, 2H, Ar-H), 3.6543-3.5906(s, 6H, Ar-3,4-$(OCH_3)_2$. Mass (LC-MS): m/z 489.18(M), 490.34(M + 1, 100%).

**Compound.II-4k:(4-{(E)}-[3-hydroxyphenyl) methylidene]amino}phenyl)(3-{(E)-[pyrazine -2yl)imino]methyl}-1H-indol-1-yl)methanone:** M.P. 229-231ºC, Mol. Formula: $C_{27}H_{19}N_5O_2$, Yield.81.91%. IR ($\nu$ cm−1): 3564(-OH *Str* in Ar-OH); 3087(C-H *Str*, Aromatic), 2987(C-H *Str*, Aliphatic), 1718(-CO *Str*, NC=O methanone); 1612(C=N, *Str*), 1532(C=CH *Str*), 1412(C=C *Str*), 1098(C-N, *Str*). $^1$H-NMR (DMSO) $\delta\delta$ ppm: 9.5674(s, 1H, Imine proton), 9.2983(s, 1H, Imine proton), 8.3213(s, 1H, Pyrazine proton); 8.2093-8.2003(d, 2H, Ar-H), 7.9983-7.8898(d, 2H, Ar-H), 7.7654(s, 1H, Indole proton); 7.5865-7.5765(d, 2H, Ar-H), 7.4094(d, 2H, Ar-H), 7.2342(s, 1H, Ar-H), 7.1009-7.0002(d, 2H, Ar-H); 6.8773-6.7123(t, 2H, Ar-H). Mass (LC-MS): m/z 445.15(M), 446.32(M + 1, 100%).

**Compound.II-4l:(4-{(E)}-[3-chlorophenyl) methylene]amino} phenyl)(3-{(E)-[pyrazine -2yl)imino]methyl}-1H-indol-1-yl)methanone:** M.P. 233-235ºC, Mol. Formula: $C_{27}H_{18}N_5OCl$, Yield.86.14%. IR ($\nu$ cm−1): 3068(C-H *Str*, Aromatic), 2983(C-H *Str*, Aliphatic), 1718(-CO Str, NC=O methanone), 1609(C=N, *Str*), 1545(C=CH *Str*), 1443(C=C *Str*), 1103(C-N, *Str*); 798(-Cl *Str*, Ar-Cl). $^1$H-NMR (DMSO) $\delta\delta$ ppm: 9.6843(s, 1H, Imine proton), 9.3032(s, 1H, Imine proton), 8.2893(s, 1H, Pyrazine proton); 8.1982-8.1098(d, 2H, Ar-H), 7.9873-7.9762(d, 2H, Ar-H), 7.7863(s, 1H, Indole proton); 7.6543-7.6023(d, 2H, Ar-H), 7.5643(s, 1H, Ar-H), 7.4291-7.4092(d, 2H, Ar-H), 7.2003-7.1982(d, 2H, Ar-H); 6.9983-6.9873(t, 2H, Ar-H). Mass (LC-MS): m/z 463.12(M), 464.21(M + 1, 100%), 465.21(M+2, 30%).

**Molecular Properties and ADME predictions:** Molecular properties of the processed ligands were studied by using Qikprop module. Qikprop module also predicts ADME profiles like blockage of HERG K+ channels, apparent Caco-2 cell permeability, brain/blood partition coefficient, apparent MDCK cell permeability, skin permeability, binding to human serum albumin, and human oral absorption of the given set of ligands [16].

**Molecular Docking Studies:** The digital structure of the epidermal growth factor receptor (EGFR) was retrieved from the Protein databank website with PDB Id: 1M17 and the structure was optimized by deleting unbound water molecules which are over 1 Å, adding hydrogen atoms to satisfy the valences, adding missing amino acids to stabilize side chains and energy of the whole structure was minimized using OPLS-2005 force field using Protein Preparation by using AUTODOCK suite of MGL Tools. Thus, structurally optimized protein structure was used to examine protein-ligand interactions of the dataset ligands using Glide Xp docking protocol.

**Pharmacological activity:**

**In-vitro Anti-Diabetics-Glucose diffusion inhibitory study:** A series of novel pyrazine fused Indole derivatives II-(4a-4l) were evaluated for antidiabetic-glucose diffusion inhibitory activity was decisive by incubating a solution of maltose substrate with Tris volume of buffer pH 8.0 and different concentrations of compounds II-(4a-4l**)** at 35$^0$C. The reaction was commencing by adding $\alpha$-glucosidase enzyme into the reaction mixture followed by incubation at 35$^0$C. Then the reaction was determined by the addition of a colorimetric reagent like DNSA [17]. Ethanol was used as control and it was prepared using the alike procedure replacing the lead molecules. The intensity of the color compounds was measured at 540nm. Finally, the percentage inhibition (I %) was calculated by using the following formula.

$$\% \text{ inhibitory activity} = (Ac\text{-}As)/Ac \times 100$$

Where Abc control is the absorbance of the control and Abs sample is the absorbance of the sample.

**In-vitro Anticancer activity- Brine Shrimp Lethality Bioassay:**

The 150 mg eggs weight of Brine shrimp (Artemia salina) were hatched in a 1liter conical shaped vessel filled with sterile artificial sea water with constant aeration for 72 hrs. Then the pH was adjusted to 8.5, to avoid risk of larvae death because of reduction in pH during incubation. Then add 15ml of 0.06% yeast solution to a vessel for every litre of salt water after 48 hrs in order to feed larvae. It takes about 72 hours for hatching. Active nauplii free from egg shells were collected and used for the Bioassay [18]. Ten active nauplii were taken into a test tube containing sample, filled with 5 ml total volume of artificial sea water. Experiment was conducted using three test tubes per 25,50 and 100µg/ml concentrations of synthesized compounds I(3a-3t). Sea water (vehicle) was used as a control and Cyclophosphamide as standard drug. After 24 hours, live nauplii were counted and $LC_{50}$ value was estimated. The percentage lethality was determined by comprising the mean surviving larvae of the test and control tubes. $LC_{50}$ values were obtained from concentration verses percentage lethality using Finney's probit statistical analysis method.

**RESULTS AND DISCUSSION**:

A series of novel pyrazine fused Indole derivatives II-(4a-4l) was prepared. It was synthesized via Schiff's base with appropriately 2-aminopyrazine followed by n-benzoylation and Schiff's base with substituted benzaldehydes. All the synthesized compounds were performed characterized by IR, $^1$HNMR and MASS spectral analysis and evaluated for their antidiabetic and anticancer activities.

**Molecular Properties and ADME predictions**: A series of novel pyrazine fused Indole derivatives II-(4a-4l) were designed and screened by make use of

various softwares like swiss ADME, PKCSM, Osiris, Mol inspiration and Molsoft. All the novel thiazole derivatives (only lead molecules) are following Lipinski rule (mol.wt below ≤500 g/mol. Various molecular properties such as molecular weight (MW), dipole, volume, solvent accessible surface area (SASA), hydrophobic component of SASA (FOSA), hydrophilic component of SASA (FISA), π (carbon and attached hydrogen) component of the SASA (PISA), and weakly polar component of the SASA (halogens, P, and S) (WPSA) have been determined using Qikprop module (Table 2).

**Table 2:** Predicted Molecular Properties of the Dataset Ligands and the Recommended Range of the Values

| Molecule | MW | Dipole | SASA | FOSA | FISA | PISA | WPSA | Volume |
|---|---|---|---|---|---|---|---|---|
| II_4a | 429.16 | 1.542 | 709.65 | 118.65 | 23.83 | 532.198 | 29.04 | 1287.64 |
| II_4b | 443.17 | 2.043 | 732.76 | 210.353 | 24.98 | 489.09 | 32.093 | 1332.443 |
| II_4c | 459.17 | 5.999 | 743.940 | 119.03 | 25.983 | 487.32 | 99.093 | 1310.733 |
| II_4d | 463.12 | 4.985 | 755.765 | 132.762 | 128.904 | 478.98 | 27.432 | 1345.094 |
| II_4e | 447.15 | 4.982 | 732.98 | 221.532 | 25.93 | 481.982 | 26.93 | 1321.983 |
| II_4f | 507.07 | 3.02 | 787.908 | 286.373 | 27.93 | 468.092 | 32.093 | 1432.09 |
| II_4g | 474.14 | 2.983 | 776.54 | 210.432 | 25.93 | 447.32 | 94.092 | 1368.903 |
| II_4h | 445.15 | 5.893 | 823.98 | 278.43 | 23.094 | 434.23 | 94.98 | 1457.143 |
| II_4i | 474.14 | 4.273 | 787.09 | 210.36 | 29.87 | 431.092 | 99.032 | 1378.564 |
| II_4j | 489.18 | 4.102 | 787.32 | 143.392 | 39.09 | 439.03 | 96.993 | 1387.833 |
| II_4k | 445.15 | 3.983 | 729.39 | 121.093 | 32.32 | 487.43 | 99.034 | 1321.432 |
| II_4l | 463.12 | 4.873 | 823.23 | 287.432 | 30.02 | 409.32 | 98.173 | 1488.432 |

**Recommended range**: MW – molecular weight (400-620), dipole (1-10.5), SASA- solvent accessible surface area (450-900), FOSA – hydrophobic component of SASA (0-650), FISA – hydrophilic component of SASA (10-280), PISA - π (carbon and attached hydrogen) component of the SASA (0.0 – 550.0), WPSA - Weakly polar component of the SASA (halogens, P, and S) (0.0 – 120.0), volume (700-2100).

The ADME Parameters such as dipole, SASA, FOSA, FISA, WPSA, and volume are also within the normal range for all the compounds. However, PISA component of certain compounds was beyond the recommended range. Predicted ADME parameters include partition co-efficient, predicted aqueous solubility (QPlogS), probability of CNS effects, blockage of HERG K+ channels (QPlogHERG), apparent Caco-2 cell permeability (QPPCaco), brain/blood partition coefficient (QPlogBB), apparent MDCK cell permeability (QPPMDCK), skin permeability (QPlogKp), binding to human serum albumin (QPlogKhsa), and human oral absorption of the given set of ligands (Table 3).

**Table 3:** Predicted Pharmacokinetic (ADME) profiles of compounds

| Molecule | CNS | QPlog Po/w | QPlogS | QPlog HERG | QPP Caco | QPlog BB | QPP MDCK | QPlog Kp | QPlog Khsa | % Human Oral Absorption |
|---|---|---|---|---|---|---|---|---|---|---|
| **II_4a** | 1 | 6.203 | -8.564 | -7.983 | 5674.43 | 0.554 | 4873.43 | -0.32 | 1.232 | 100 |
| **II_4b** | 2 | 5.872 | -7.983 | -7.293 | 51982.33 | 0.421 | 5202.34 | -0.773 | 0.653 | 100 |
| **II_4c** | 1 | 5.232 | -8.365 | -7.453 | 5873.64 | 0.540 | 12832.3 | -0.453 | 1.673 | 100 |
| **II_4d** | -1 | 6.091 | -8.093 | -7.984 | 784.43 | -0.784 | 564.432 | -2.089 | 1.203 | 94.2 |
| **II_4e** | 2 | 6.032 | -7.893 | -7.672 | 6091.32 | 0.324 | 51293.23 | -0.290 | 0.983 | 100 |
| **II_4f** | 2 | 5.872 | -7.832 | -7.109 | 57643.4 | 0.543 | 3894.343 | -0.493 | 1.563 | 100 |
| **II_4g** | 1 | 6.563 | -8.984 | -7.763 | 6778.34 | 0.435 | 787.4 | -0.344 | 1.43 | 100 |
| **II_4h** | 1 | 5.982 | -10.632 | -7.982 | 5866.43 | 0.509 | 10000 | -0.560 | 1.984 | 100 |
| **II_4i** | 2 | 6.093 | -8.983 | -7.032 | 5453.342 | 0.498 | 10000 | -0.409 | 0.873 | 100 |
| **II_4j** | -1 | 5.892 | -11.92 | -7.763 | 874.453 | -0.732 | 1293.433 | -3.983 | 1.332 | 97.67 |
| **II_4k** | 0 | 6.872 | -10.03 | -7.209 | 5352.344 | 0.584 | 3742.43 | -0.432 | 1.894 | 100 |
| **II_4l** | 2 | 6.342 | -9.043 | -7.653 | 5983.043 | 0.453 | 983.244 | -0.652 | 0.984 | 100 |

**Recommended range:** CNS Predicted central nervous system activity on a –2 (inactive) to +2 (active) scale; QPlogPo/w: Predicted octanol/water partition coefficient ( –2.0 - 6.5); QPlogS: Predicted aqueous solubility (-7.8 – 0.5); QPlogHERG: Predicted IC50 value for blockage of HERG K+ channels (below -6); QPPCaco: Predicted apparent Caco-2 cell permeability in nm/sec. Caco- 2 cells are a model for the gut-blood barrier (<25: poor, >500: great); QPlogBB: Predicted brain/blood partition coefficient (-1 – 2.5); QPPMDCK: Predicted apparent MDCK cell permeability in nm/sec. MDCK cells are considered to be a good mimic for the blood-brain

barrier (<25: poor, >500: great); QPlogKp: Predicted skin permeability, log Kp (–504 – – 0.32); QPlogKhsa: Prediction of binding to human serum albumin (–1.8 – 1.2); %Human- Oral Absorption (>90% is high, <30% is poor).

**Molecular docking studies**: Molecular docking studies were performed in order to find the possible protein ligand interactions of the dataset ligands. Additionally, these also assisted in identifying the conformational changes of the ligand in the protein environment. About 100 different protein-ligand complex conformations for each docked complex were generated through Glide XP module; the confirmation with highest EModel energy was only displayed in the result. Glide dock sores of the dataset ligands were shown in Table 4 along with the interaction amino acids and number of amino acids.

**Table 4.** Molecular docking interactions with EGFR kinase domain

| Compound No | Dock score XP GScore | No of H-bonds | Interacting amino acids | H-bond lengths (Å) |
|---|---|---|---|---|
| **II-4a** | **-9.2** | 1 | LEU:694, PHE:699, VAL:702, LYS:721, ASP:831 | 2.53 |
| **II-4b** | **-8.3** | 0 | LEU:694, PHE:699, VAL:702, | - |
| **II-4c** | **-9.1** | 1 | LEU:694, PHE:699, VAL:702, LYS:721, ASP:831 | 2.37 |
| **II-4d** | **-9.1** | 1 | LEU:694, PHE:699, VAL:702, LYS:721, ASP:831 | 1.87 |
| **II-4e** | **-7.4** | 0 | LEU:694, , VAL:702, LYS:721, ASP:831 | - |
| **II-4f** | **-8.9** | 1 | LEU:694, PHE:699, VAL:702, LYS:721, | 2.21 |
| **II-4g** | **-9.1** | 1 | PHE:699, VAL:702, LYS:721, | 2.122 |
| **II-4h** | **-9.2** | 1 | LEU:694, PHE:699, VAL:702, LYS:721, ASP:831 | 2.34 |
| **II-4i** | **-6.4** | 0 | VAL:702, LYS:721, ASP:831 | - |
| **II-4j** | **-7.6** | 1 | LEU:694, PHE:699, VAL:702, LYS:721 | 1.45 |
| **II-4k** | **-5.2** | 1 | LEU:694, PHE:699, LYS:721, ASP:831 | 1.98 |
| **II-4l** | **-7.4** | 0 | PHE:699, VAL:702, LYS:721, ASP:831 | - |

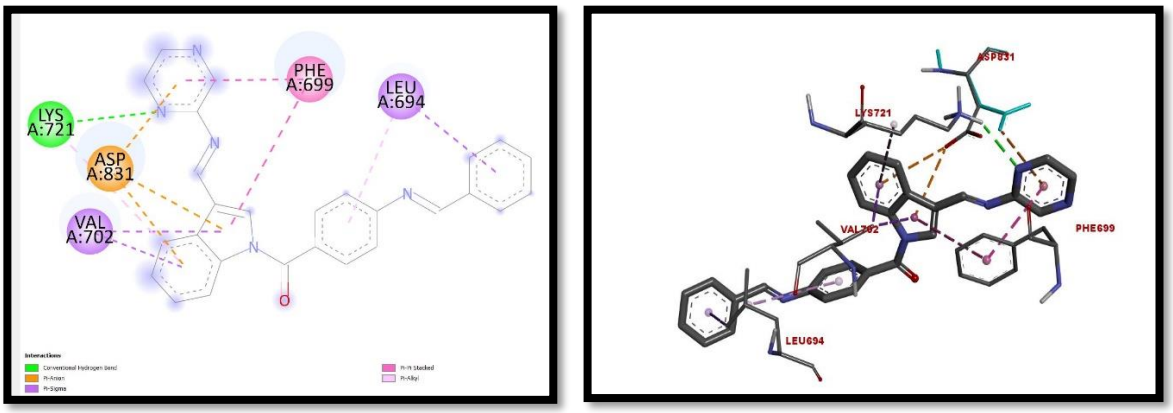


**Compound-II-4a: 2d dock and 3d dock**

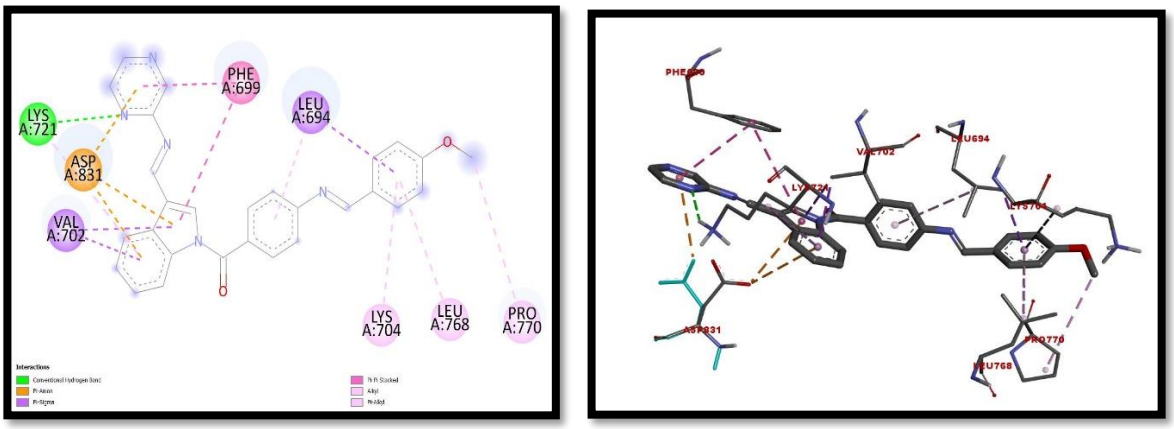


**Compound-II-4c: 2d dock and 3d dock**

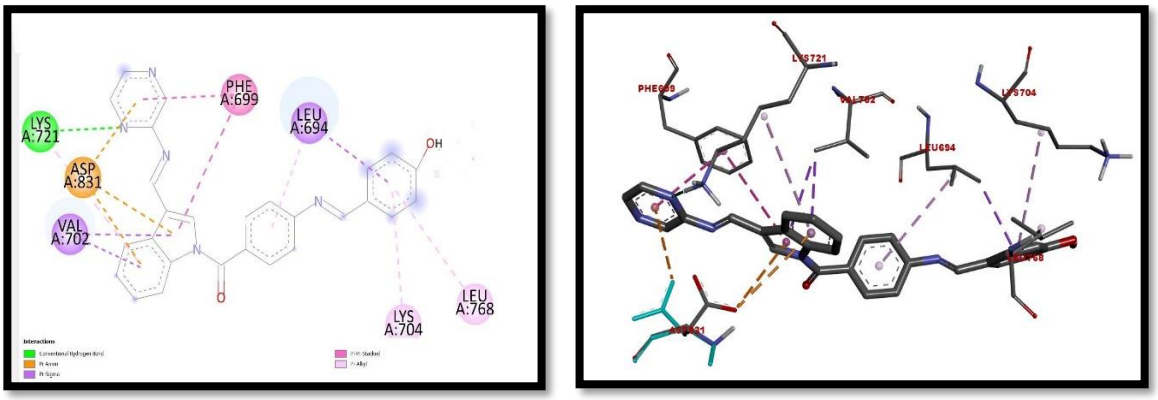


**Compound-II-4h: 2d dock and 3d dock**

**Figure.2.** Docking Pose between the Ligand and the Protein. (Dock1 and Dock-2 for designed molecules)

**Antidiabetic activity:** The antidiabetic activity (Glucose diffusion inhibitory study) of novel pyrazine fused indole derivatives results were recorded in table no.5.

The compound II-4c and II-4h has shown significant antidiabetic activity due to the presence of electrophilic groups compared with standard drug Acarbose. The compound II-4c (58.93µg/ml) and II-4h (47.82 µg/ml) has shown highest IC50 values than other compounds.

**Table.No.5.** Antidiabetic activity (Glucose diffusion inhibitory study) of novel pyrazine fused indole derivatives-(II-4a, II-4c, II-4d, II-4e, II-4f, II-4h, II-4i, and II-4l).

| Samole Name | $IC_{50}$ (µg) |
|---|---|
| **II-4a** | 67.83 |
| **II-4c** | **58.93** |
| **II-4d** | 62.32 |
| **II-4e** | 66.32 |
| **II-4f** | 53.7 |
| **II-4h** | **47.82** |
| **II-4i** | 76.21 |
| **II-4l** | 82.34 |
| **Acarbose** | **33.84** |

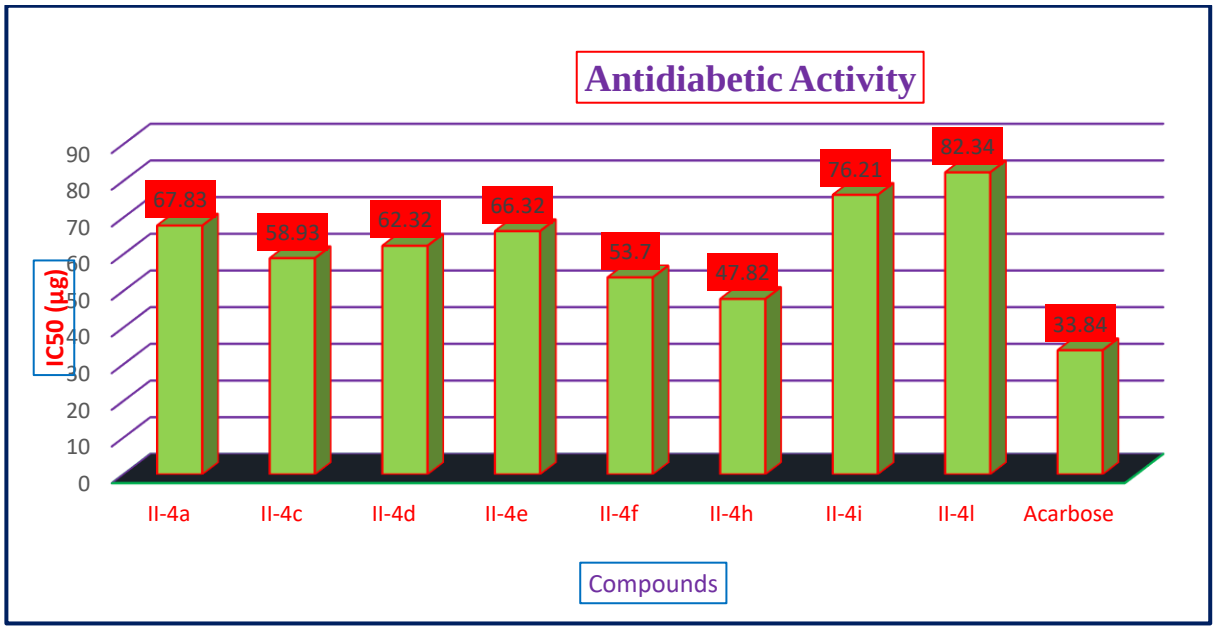


**Figure 3:** Graphical representation of Antidiabetic activity (Glucose diffusion inhibitory study) of compounds-(II-4a, II-4c, II-4d, II-4e, II-4f, II-4h, II-4i, and II-4l).

**Anticancer activity:** For anticancer activity (Brine shrimp lethality activity) of synthesized molecules was found to be directly proportional to the concentration of the synthesised compounds.

The novel pyrazine fused indole compound II-4c (56.68µg/ml) and II-4h (38.08µg/ml) were shown more potent $IC_{50}$ value (Table no 6) compared with standard cyclophosphamide (21.32µg/ml).

**Table.No.6.** Anticancer activity (Brine Shrimp Lethality Bioassay) of compounds-(II-4a, II-4c, II-4d, II-4e, II-4f, II-4h, II-4i, and II-4l).

| S.No | Compounds | Concentrations (µg/ml) | No of Shrimp tested | Average Mortality after 24hr. | Percent Mortality | LC50 (µg/ml) |
|---|---|---|---|---|---|---|
| **1** | **Control** | 00 | 10 | 00 | 00 | 0 |
| **2** | **II-4a** | 20 | 10 | 02 | 10 | 138.33 |
| | | 50 | 10 | 03 | 30 | |
| | | 100 | 10 | 04 | 40 | |
| **3** | **II-4c** | 20 | 10 | 01 | 10 | **56.68** |
| | | 50 | 10 | 04 | 40 | |
| | | 100 | 10 | 05 | 50 | |
| **4** | **II-4d** | 20 | 10 | 01 | 10 | 127.28 |
| | | 50 | 10 | 02 | 20 | |
| | | 100 | 10 | 04 | 40 | |
| **5** | **II-4e** | 20 | 10 | 01 | 10 | 100.79 |
| | | 50 | 10 | 03 | 30 | |
| | | 100 | 10 | 05 | 50 | |
| **6** | **II-4f** | 20 | 10 | 01 | 10 | 179.16 |
| | | 50 | 10 | 02 | 20 | |
| | | 100 | 10 | 03 | 30 | |
| **7** | **II-4h** | 20 | 10 | 04 | 40 | **38.01** |
| | | 50 | 10 | 06 | 60 | |
| | | 100 | 10 | 07 | 70 | |
| **8** | **II-4i** | 20 | 10 | 03 | 30 | 175.52 |
| | | 50 | 10 | 04 | 40 | |
| | | 100 | 10 | 04 | 40 | |
| **9** | **II-4l** | 20 | 10 | 01 | 10 | 128.73 |
| | | 50 | 10 | 02 | 20 | |
| | | 100 | 10 | 04 | 40 | |
| **11** | **Cyclophos phamide** | 20 | 10 | 05 | 50 | 21.34 |
| | | 50 | 10 | 06 | 60 | |
| | | 100 | 10 | 08 | 80 | |

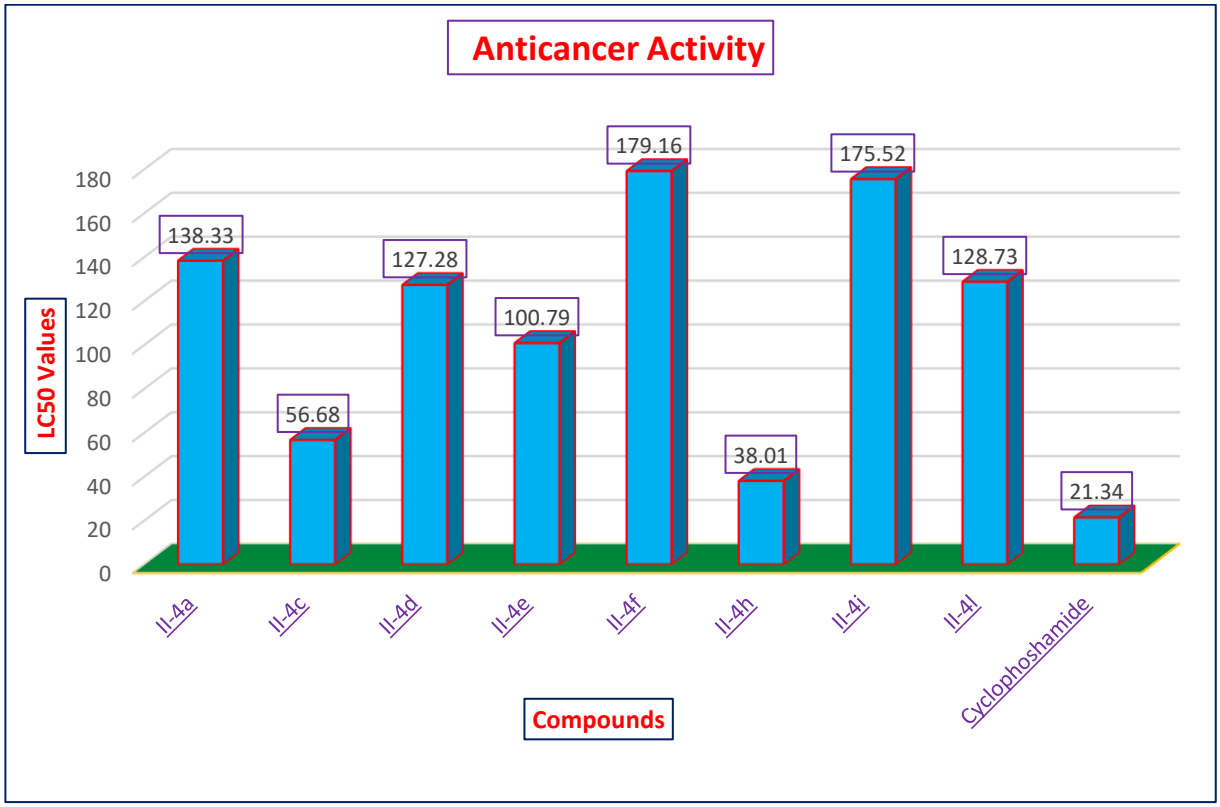


**Figure 4:** Graphical representation of Anticancer activity (Brine Shrimp Lethality Bioassay) of compounds-(II-4a, II-4c, II-4d, II-4e, II-4f, II-4h, II-4i, and II-4l).

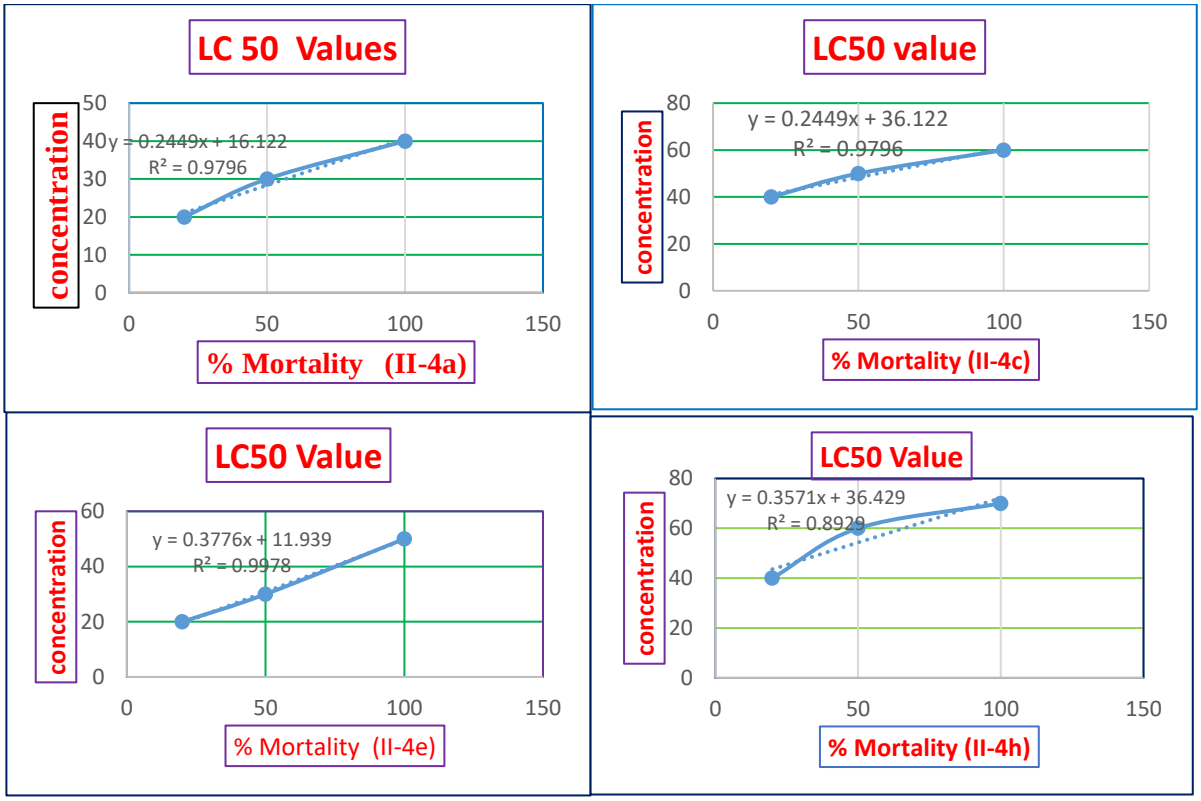


**Figure 5:** Graphical representation of Anticancer Activity-Brine Shrimp Lethality Bioassay of lead molecules-$LC_{50}$ values.

**CONCLUSION:** A series of novel pyrazine fused Indole derivatives II-(4a-4l) were synthesized and characterized by physical and spectral analysis. All the synthesized compounds were showing significant antidiabetic, anticancer activities and finally performed by Molecular docking studies.

**ACKNOWLEDGMENTS:** The authors are grateful to the Head, Deportment of Chemistry, Deportment of Pharmacy, College of Pharmaceutical Sciences, Puri, India for providing the laboratory facilities.

**CONFLICT OF INTEREST:** The authors declare that they have no conflict of interest. The authors alone are responsible for the content and writing of the paper.

**REFERENCES**

1. Vargas, E.; Echeverri, F.; Upegui, Y.A.; Robledo, S.M.; Quiñones, W. Hydrazone derivatives enhance antileishmanial activity of thiochroman-4-ones. Molecules. 2017; 3(1), 70-81.
2. Meira, C.S.; Dos Santos Filho, J.M.; Sousa, C.C.; Anjos, P.S.; Cerqueira, J.V.; Dias Neto, H.A.; da Silveira, R.G.; Russo, H.M.; Wolfender, J-L.; Queiroz, E.F.; Moreira, D.R.M.; Soares, M.B.P. Structural design, synthesis and substituent effect of hydrazone-Nacylhydrazones reveal potent immunomodulatory agents. Bioorg. Med. Chem., 2018, 26(8), 1971-1985.
3. Turan-Zitouni, G.; Hussein, W.; Sağlık, B.N.; Tabbi, A.; Korkut, B. Design, synthesis and biological evaluation of novel N-pyridylhy drazone derivatives as potential monoamine oxidase (MAO) inhibitors. Molecules. 2018; 23(1), 113.
4. MS. Ahmad, B. Mirza, Synthesis, chemical characterization and biological screening for cytotoxicity and antitumor activity of Organotin(IV) derivatives of 3,4-Methylenedioxy 6-nitrophenylpropenoic acid. Molecules. 2007; 12(23): 2348-63.
5. Gang Chen, Ye Wang, Xiaojiang Hao, M. Shuzhen, S. Qianyun. Simple isatin derivatives as free radical scavengers: synthesis, biological evaluation and structure-activity relationship. Chem Cent J, 37(5): 165-574(2017).
6. R.F. Costa, L.C. Turones, K.V.N. Cavalcante, I.A. Rosa Jr., C.H. Xavier, L.P. Rosseto, H.B. Napolitano, P.F. da Silva Castro, M.L.F. Neto, G.M. Galvão, R. Menegatti, G.R. Pedrino, E.A. Costa, J.L.R Martins and J.O. Fajemiroye, Front. Pharmacol. 2021; 12, 666725.
7. Pomel S, Dubar F, Forge D, Loiseau PM, Biot C. New heterocyclic compounds: synthesis and antitrypanosomal properties. *Bioorg Med Chem*. 2015; 23: 5168–5174.

8. Singh P, Kumari K, Awasthi SK, Chandra R. Virtual screening and docking studies of synthesised chalcones: potent anti-malarial drug. *Int J Drug Dev Res*. 2016; 8:49–56.
9. Muhammed MT, Aki-Yalcin E. Homology modeling in drug discovery: overview, current applications, and future perspectives. *Chem Biol Drug Des*. 2019: 93:12–20.
10. Guilherme, F.D.; Simonetti, J.É.; Folquitto, L.R.S.; Reis, A.C.C.; Oliver, J.C.; Dias, A.L.T.; Dias, D.F.; Carvalho, D.T.; Brandão, G.C.; de Souza, T.B. Synthesis, chemical characterization and antimicrobial activity of new acylhy drazones derived from carbohydrates. J. Mol. Struct., 2019; 1184: 349-356.
11. Ugwu DI, Okoro UC, Ukoha PO, Okafor S, Ibezim A, Kumar NM. Synthesis, characterisation, molecular docking and in vitro antimalarial properties of new
12. carboxamides bearing sulphonamide. *Eur J Med Chem*. 2017; 35: 349–369.
13. Patel B, Singh V, Patel D. Structural Bioinformatics. In: Shaik, NA, Hakeem, KR, Banganapalli, B, et al., eds. *Essentials of Bioinformatics*, vol. I. Cham, Switzerland: Springer; 2019; 169–199.
14. Sainy J, Sharma R. Synthesis, antimalarial evaluation and molecular docking studies of some thiolactone derivatives. *J Molec Struct*. 2017; 1134:350–359.
15. V.S. Tangeti, R. Varma K, G.V. Siva Prasad and K.V.V.V. Satyanarayana, Synth. Commun. 2016; 46: 613.
16. Mohanty D, Gilani SJ, Zafar A, Imam SS, Kumar LA, Ahmed MM, Jahangir MA, Bakshi V, Ahmad W, Eltayib EM. Formulation and Optimization of Alogliptin-Loaded Polymeric Nanoparticles: In Vitro to In Vivo Assessment. Molecules. 2022 Jul 13;27(14):4470.
17. L. De la Cruz-Martínez, C. Duran-Becerra, M. González-Andrade, J.C. Páez-Franco, J.M. Germán-Acacio, J. Espinosa-Chávez, J.M. TorresValencia, J. Pérez-Villanueva, J.F. Palacios-Espinosa, O. Soria-Arteche and F. Cortés-Benítez, Molecules. 2021; 26, 4375.
18. S. Raghavendra Prasad, N. D. Satyanarayan, A. Satish Kumar Shetty, Harishkumar Shivanna, B. Thippeswamy. Design and Synthesis of Some 1,3,4-Thiadiazole Amines: Molecular Docking, in silico ADMET, in vitro Antimicrobials and Antioxidant Studies. Asian Journal of Chemistry; 34(8), 2067-2073, (2022).
19. G. Ganga Reddy, S. Ramakrishna Reddy, Ch. Venkata Ramana Reddy, E. Laxminarayana, B. Srinivasa Reddy. Synthesis, Characterization and Molecular Docking Studies of 5-Chloro-1-(1H-indole-2-yl)-3-methyl-4,5-dihydro-1H-pyrazole-4-carboxylic Acids. Asian Journal of Chemistry; 34(7), 1639-1643, (2022).